# TeV photons and Neutrinos from giant soft-gamma repeaters flares

Francis Halzen<sup>a</sup>, Hagar Landsman<sup>a</sup>, Teresa Montaruli<sup>a,b,\*</sup>

<sup>a</sup> University of Wisconsin, Chamberlin Hall, Madison, WI 53706 <sup>b</sup> On leave of absence from Universitá di Bari and INFN

# Abstract

During the last 35 years three giant flares were observed from so-called Soft Gamma Repeaters (SGR's). They are assumed to be associated with star-quakes of pulsars accelerating electrons and, possibly, protons to high energy in the huge magnetic fields as inferred from the observations. Because of this and the observation of non-thermal emission it has been speculated that they may be cosmic ray accelerators producing gamma-rays up to TeV energies. Neutrino telescopes, such as AMANDA and the ANTARES now under construction, could be used as TeV- $\gamma$  detectors for very short emissions by measuring underground muons produced in  $\gamma$  showers. We estimate signal and background rates for TeV photons from SGR giant flares in AMANDA, and we provide an estimate of the gamma shower events that Milagro could detect.

Moreover, we consider that, if hadrons are accelerated in these sources, high energy neutrinos would be produced together with photons. These may be detected in neutrino telescopes using neutrino-induced cascades and upgoing muons.

We argue that the Antarctic Muon and Neutrino Detector Array AMANDA may have observed the December 27, 2004 giant flare from the soft gamma-ray repeater SGR 1806-20 if the non-thermal component of the spectrum extends to TeV energies (at present the actual data is subject to blind analysis). Rates should be scaled by about two orders of magnitude in km<sup>3</sup> detectors, such as IceCube, making SGR flares sources of primary interest.

Email addresses: halzen@pheno.physics.wisc.edu (Francis Halzen), hagar.landsman@icecube.wisc.edu (Hagar Landsman), tmontaruli@icecube.wisc.edu (Teresa Montaruli).

<sup>\*</sup> Corresponding author.

#### 1 Introduction

Soft gamma repeaters are X-ray pulsars that sporadically emit energies typically of the order of  $10^{41}D_{10}^2$  ergs in X-rays and soft  $\gamma$ -rays, with the distance D in units of 10 kpc, in short bursts lasting hundreds of milliseconds [1,2]. Their steady emission is periodic with typical periods of 5-10 seconds and luminosities between  $10^{35} \div 10^{36}$  ergs/s. These objects are thought to be magnetically-powered spinning neutron stars also known as magnetars.

The first SGR was observed on Jan. 7, 1979 when a burst of soft gamma-rays, lasting about 0.25 s, was detected by the Venera space-craft from SGR 1806-20 [1]. To date five SGR's have been identified. The giant bursts are thought to result from the rearrangement of the huge magnetic field inferred to be of the order of  $B \sim 10^{15}$  Gauss from their spin down rates [3]. Star-quakes are thought to fracture the rigid crust and cause these outbursts. The flares result from the formation and dissipation of strong localized currents resulting from magnetic field rearrangements associated with the quakes.

SGR's have been classified as separate phenomena from gamma-ray bursts (GRB's) and anomalous X-ray pulsars (AXP's) [4] despite similarities. SGR bursts are less frequent than GRB's and, unlike GRB's, they do repeat and show clear periodicity. It is not excluded however that at least some of the short GRB's are extra-galactic SGR's and, vice-versa, that some of the intense flares of SGR's are galactic GRB's. SGR's are very similar to the 8 observed AXP's, the main difference being the lack of bursts for the latter. Recently, though, SGR-like bursts were observed from at least one, and possibly two AXP's [4]. Hence SGR's and AXP's might belong to the same class of neutron stars.

Like GRB's, SGR's also produce non-thermal radiation during the short bursts. Because of this and the large luminosities produced, it has been speculated that these objects accelerate cosmic rays to high energy. The sudden changes of the large magnetic fields would accelerate protons or nuclei that produce neutral and charged pions in interactions with thermal radiation. These would be the parents of gamma-rays and neutrinos reaching high energies.

We here propose that these high energy gamma-rays can be detected by underground neutrino telescopes and by experiments, such as Milagro [5] and the Tibet array [6]. (The premier instruments for TeV gamma-ray detection, air Cherenkov telescopes, must point at an SGR in order to detect it and this is unlikely for such a serendipitous event.) Underground detectors have the capability to detect high energy muons produced in air showers initiated by TeV-energy gamma-rays at the top of the atmosphere. Though gamma-ray showers are muon-poor, the large number of secondary photons produced will

occasionally produce pions rather than electron-positron pairs. These decay into muons that can reach large underground detectors such as Baikal [7], AMANDA/IceCube [8,9] and future Mediterranean detectors [10,11,12,13].

TeV gamma-rays could be produced in electromagnetic process and also in hadronic interactions on the thermal radiation, and in this case they would be accompanied by a flux of neutrinos. A model for neutrino production from magnetars in their steady phase of periodic emission has been proposed [14]. Here we concentrate instead on the possibility that short bursts of neutrinos are produced during the rare violent giant flares. Because of the negligible background during the short time and in the direction of the SGR, the instruments have a much larger sensitivity for such events.

This paper is organized as follows: in Sec. 2 we review the photon observations of the giant flares. In Sec. 3 we argue that they should produce detectable events in earth-based experiments provided their spectra extend to TeV energies not accessible to satellites. For illustration we calculate the rates of muons from gamma showers on Milagro surface [5] and the number of muons from gamma showers reaching the AMANDA detector [8]. In Sec. 4 we estimate the number of upward-going muons and showers produced by neutrinos in the same detector. Similar rates are expected in neutrino telescopes of similar depth such as ANTARES [10].

## 2 Giant bursts from Soft Gamma Repeaters: Observations

In recent years SGR giant bursts have been observed from 3 objects: SGR 0526-66 on May 5, 1979, SGR 1900+14 on August 27, 1998 and SGR 1806-20 on December 27, 2004 [1]. Their UT times and equatorial coordinates are given in Tab. 1.

Source	RA	Declination	Distance	UT
	(J2000)	(J2000)	(kpc)	
SGR 0526-66	$05^h 26^m 00.89^s$	$-66^{\circ}04^{'}36.3^{''}$	50	May 5, 79 15:51
SGR 1900+14	$19^h 07^m 14.24^s$	$+09^{\circ}19^{'}20.1^{''}$	14.5	Aug. 27, 98 10:22:15.7
SGR 1806-20	$18^h 08^m 39.32^s$	$-20^{\circ}24^{'}39.5^{''}$	15.1	Dec. 27, 04 21:30:26.65

Table 1

Coordinates and UT times of the giant flares [1]. UT time for SGR 1900+14 is from [15] and for SGR 1806-20 from [16]. Positions (right ascension RA and declination) and distances are from [17] for SGR 1900+14 and from [18] and [19] for SGR 1806-20, respectively.

Giant flares are distinguished from common SGR bursts by their extreme

energies ( $\sim 10^{44}$  ergs/s) emitted during the first second followed by subsequent emission lasting several minutes showing pulsations associated with the neutron star. While the total energy emitted is 6-7 orders of magnitude less intense than for GRB's, their distance is typically a factor of  $10^5$  smaller resulting in a flux increased by a factor  $10^{10}$  relative to cosmological GRB's. The opportunity for a detection is obvious.

The bulk emission of SGR's can be routinely explained by Optically Thin Thermal Bremsstrahlung (OTTB). We focus on the non-thermal component observed in giant flares with a hard power law (PL) spectrum,  $\frac{dN}{dE} \propto E^{-1.5}$  [1,15]. This is harder than the Band spectrum observed for a typical GRB [20]. Because of the energetics and the non-thermal spectra giant flares should be prime suspects for accelerating cosmic rays and for producing associated fluxes of photons and neutrinos of TeV-energy, possibly higher.

An interesting feature is that both SGR 1900+14 and SGR 1806-20 are associated with clusters of massive stars [1,17,19], while the other giant flare emitter, SGR 0526-66, is associated with the supernova remnant N49 in the Large Magellanic Cloud. It has been suggested that association of massive stars, such as Cygnus OB2, can host highly magnetized pulsars that accelerate heavy nuclei up to high energies [21]. TeV  $\gamma$ 's and  $\nu$ 's can be produced by cosmic rays by interacting with the innermost parts of the winds of massive O and B stars [22]. Moreover, relativistic nuclei photo-disintegrate in the intense radiation fields producing neutrinos from the decay of neutrons [23]. For a review of galactic neutron stars in high density environments: see [24]. In a recent paper [25] it has also been suggested that the December 27, 2004 flare has similar features to a GRB and can be similarly explained as a relativistically expanding fireball with baryon loading. Proton acceleration will inevitably lead to neutrino emissions.

The December 27, 2004 flare exceed previous flares in intensity by over one order of magnitude. It was initially detected by INTEGRAL [16], then by Konus-Wind [26] and later by RHESSI [27]. While the germanium detectors operating from 3 keV to 15 MeV were saturated, RHESSI measured the flux using the particle detector with a time resolution of 0.125 s in two energy channels with thresholds of 65 keV and 650 keV. These data indicate significant emission above 650 keV for  $\sim 0.25$  s during the giant flare. A conservative lower limit on the total fluence of the primary giant peak is 0.1 ergs/cm<sup>2</sup>, more than one order of magnitude larger than reported for SGR 1900+14 (5.5 · 10<sup>-3</sup> ergs/cm<sup>2</sup> in the first  $\sim 0.35$  s [28]). Assuming a distance of  $\sim 15$  kpc for SGR 1806-20 [19] and isotropic emission, a lower limit on the total hard X-ray/gamma-ray energy released is  $8 \cdot 10^{45}$  ergs during the giant flare.

So far no spectral analysis has been reported for the 27 Dec., 2004 giant flare during which the AMANDA neutrino telescope was taking data. In Sec. 2.1

we study instead the features of the giant flare SGR 1900+14 on August 27, 1998 during which the AMANDA detector had been partially completed and and was taking data with 10 strings; we refer to it as AMANDA B-10.

# 2.1 The features of the SGR 1900+14 giant flare

SGR 1900+14 was first observed in Jan. 1979 in the Aquila constellation. Thought initially to be located near SNR G42.8+0.6 at  $\sim 5$  kpc, it is now believed to be associated with a massive star cluster at 14.5 kpc [17]. The position of the persistent emitter is given in Tab. 1 [17]. Its period of steady X-ray emission is 5.16 s with a luminosity of the order of  $2-3.5\cdot 10^{35}$  ergs/s. The quiescent energy spectrum can be fitted by a Black Body (BB) function with a temperature of 0.43 keV and a Power Law (PL) shape with a negative spectral index in the range  $-1.0 \div -2.5$  [1]. Various flares with peak luminosities between  $10^{38} \div 10^{41}$  ergs/s and durations of the order of 0.1 s have been observed. SGR 1900+14 emitted a giant flare on Aug. 27, 1998 [15,28,29,30]. Two relatively high fluence events occurred on Aug. 29, 1998 [31] and on Apr. 28, 2001 [32]. For reasons already explained in Sec. 2, we focus on the giant flare whose spectral properties have been well studied, including those of the hard non-thermal component [15,30].

Most information on the giant flare comes from Beppo-SAX [15,30], Konus-Wind [28] and Ulysses [29]. All suffer from saturation problems during the first second of the burst. Unfortunately, there are no clear spectral measurements covering the first  $\sim 0.35$  s above 250 keV. Konus-Wind reported spectra below 250 keV for the first second of the emission; see Fig. 1 [28]. Also shown is the counting rate showing the saturation of the detector. Konus-Wind spectra can be described by a OTTB spectrum typical of electromagnetic processes because it was not sensitive to the high energy component.

The energy and fluence measurements are also complicated by pile-up and dead time problems. Mazets et al. [28] find a lower limit to the fluence in the first  $\sim 0.35 \text{ s}$  of  $5.5 \cdot 10^{-3} \text{ ergs/cm}^2$  for  $E_{\gamma} > 15 \text{ keV}$ . For a source at 14.5 kpc and isotropic emission this corresponds to a lower limit on the total energy emitted by the source of  $1.4 \cdot 10^{44}$  ergs during the peak of the burst. A similar amount of energy was emitted in the long tail with an exponential decay of  $\sim 90 \text{ s}$  that followed the burst and lasted several hundreds of seconds.

Similar conclusions can be inferred from the Ulysses data [29] that were even more affected by saturation because of its sensitivity in the interval 25-150 keV.

We next concentrate on the Beppo-SAX data with energy up to 700 keV.

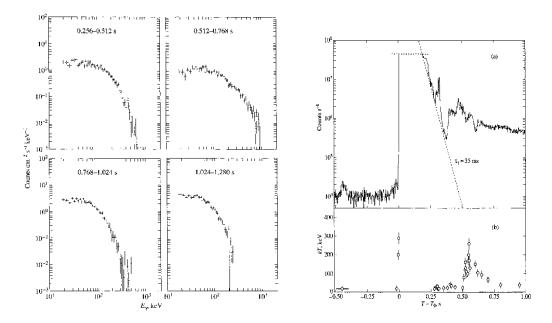


Fig. 1. On the left: Spectra measured by Konus-Wind in 4 time intervals of the initial emission. On the right: Counting rate during the first second of the burst for  $E_{\gamma} > 15$  keV and parameter kT of the OTTB law  $E^{-1}e^{-E/kT}$  that fits the energy spectra on the left as a function of time. Figures from [28].

# 2.2 Beppo-SAX observations of the Aug. 27, 1998 giant flare

Beppo-SAX data on SGR 1900+14 were first published in [15] and updated in [30]. Data from the Beppo-SAX Gamma-Ray Burst Monitor (GRBM) were also affected by saturation and only a lower limit on the fluence is reported for the first 68 s of the flare. The experiment could not determine the event rise-time for timescales shorter than 1 s. Fig. 2 shows the counting rate as well as the energy spectra corresponding to 3 different time intervals in the 70-650 keV interval. Most importantly, the experiment provides information during the first 68 s where the data exhibit a very hard non-thermal component. The results were updated in [30] for a better understanding of the response of the GRBM. The energy range was extended to 40-700 keV.

Possible fits to the data are presented in Fig. 3. The published best fit is a sum of 3 functions given in Tab. 2. We have instead chosen to adopt the previous fit in Feroci *et al.*, also shown in Fig. 3, because it gives a better description of the high energy component to which we are mostly interested in this work. The data are fit with OTTB + PL, while in the more recent paper a thermal bremsstrahlung spectrum (based on [33])+ BKNPL + PL (with positive spectral index, probably an artifact of the large errors in the interval fitted) was adopted. The  $\chi^2$  of the OTTB+PL is worse because the low energy part of the spectrum is poorly fitted by the 2 functions compared to the BREM+BKNPL+PL fit. We also note that in the updated analysis the

systematic error was reduced from 10% to 2% in [15] in the low energy range and the minimum considered energy was decreased from 70 keV to 40 keV.

The total fluence corresponding to the 3 intervals is: > 6.4 for interval A  $^1$ , 2.1 for interval B and 0.49 for interval C, in units of  $10^{-4}$  erg/cm<sup>2</sup>. Assuming an isotropic emission, the energy emitted by a source at 15.1 kpc is: > 1.7, 0.6, 0.1 in units of  $10^{43}$  erg. As already observed, the value in the first interval is smaller than the one reported by Konus-Wind for the first 0.35 s [28].

For further calculations we will adopt a differential energy spectrum for E > 250 keV of  $\frac{dN}{dE} \propto E^{-1.47}$ . We will study variations of the PL spectral index to allow for the uncertainties; see Fig. 4. Moreover, since typical Fermi acceleration processes are characterized by an  $E^{-2}$  spectrum, and given the suggestion that SGR 1806-20 may be a soft GRB [25], we also consider this assumption for the spectral shape. Our different assumptions are summarized in Tab. 3. Also given is the fraction of the fluence in the PL component relative to the total fluence measured by Beppo-SAX. From Fig. 4 it is clear that the different functions adequately fit the data that were initially fitted as  $(16 \cdot (E/\text{keV})^{-1.47} \text{ keV}^{-1} \text{ cm}^{-2} \text{ s}^{-1})$ . For each spectral shape, the normalization was chosen so that the fluence in the interval 200-500 keV is the same as for the  $E^{-1.47}$  fit in [15].

$1.1 \cdot 10^3 E^{-1} e^{-\frac{E}{40.3}}$	+	$3.8 \cdot 10^{-4} E^{1.79} \ (E < 71 keV)$	+	$8.0 \cdot 10^{-10} E^{+2.14}$
		$2.2 \cdot 10^6 E^{-3.48} \ (E > 71 keV)$		
BREMS	+	BKNPL	+	$\operatorname{PL}$
192.8	$E^{-1}e^{-}$	E/55 +	16.0 <i>E</i>	$E^{-1.47}$
(	ттв	+	Р	PL

Table 2

Functions used by Guidorzi *et al.* (BREMS+BKNPL+PL) [30,34] and by Feroci *et al.* (OTTB+PL) [15,34] to fit the spectrum for the first 68 s of the flare, respectively in the energy ranges 70-650 keV and 40-700 keV (see Fig. 3). Energy is in keV.

#### 3 TeV-Gamma Showers and Induced Underground Muons

High energy gamma-rays initiate electromagnetic showers in the atmosphere via the dominant processes of bremsstrahlung and pair production. With the development of the shower a large population of photons emerges that have a probability to produce a pion rather than an electron pair. Such pions decay into muons that, with sufficient energy, can penetrate to the depth of an

Notice that this number is obtained as the integral of the functions in Tab. 2 multiplied by the duration of the burst  $\Delta t = 68$  s.

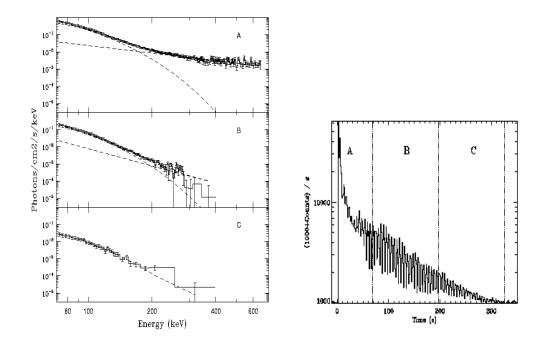


Fig. 2. On the left: Beppo-SAX counting rate during the SGR 1900+14 flare: the 3 intervals where the spectral analysis is done are 0-67 s (interval A), 68-195 s (interval B) and 196-323 s (interval C). On the right: The spectra for the 3 time intervals in the energy range of 40-700 keV. The best fit functions are shown too (figures from [15]).

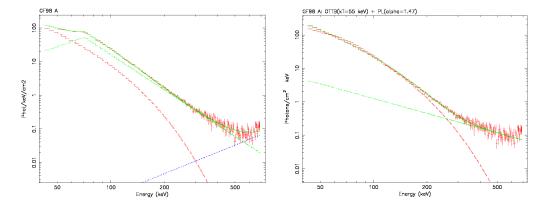
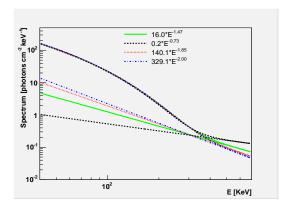


Fig. 3. On the left: Best fit to the spectrum measured by *Beppo*-SAX during the first 68 s of the flare (referred to as GF98 A in the plots) in the 40-700 keV range. On the right: fit using the Feroci *et al.* OTTB+PL function [15,34]. The corresponding fit functions are given in Tab. 2. Courtesy of C. Guidorzi [34].

underground detector. The fact that the process is rare is compensated by the large area of a detector such as AMANDA [35,36,37]. The showers can also be directly observed by ground-based wide field of view gamma detectors such as Milagro [35].

The high energy muons can be detected by deep under-ice/water neutrino tele-



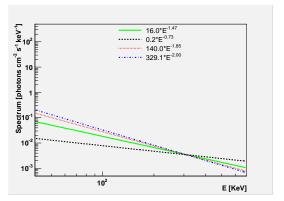


Fig. 4. On the left: Upper curve consists of the OTTB with kT = 55 keV + the 4 different PL components. Units are the same as in Beppo-SAX paper,  $keV^{-1}$  cm<sup>-2</sup> [30]. This plot shows that the different PL components do not alter much the total spectrum at low energy. As a matter of fact all different PL's added to the OTTB component overlap (see upper curves). On the right: Detail of the PL functions in the units used in this paper of  $keV^{-1}$  cm<sup>-2</sup> s<sup>-1</sup> as photon differential energy spectra for further estimates.

Energy Spectrum	Fraction of measured fluence in 68 s
$({ m keV^{-1}\ s^{-1}\ cm^{-2}})$	
$0.2 \times (E/keV)^{-0.73}$	12.9%
$16.0\times(\mathrm{E/keV})^{-1.47}$	12.2%
$140.0 \times (E/keV)^{-1.85}$	14.8%
$329.1 \times (E/keV)^{-2.00}$	16.0%

Table 3

Differential photon energy spectra assumed in this paper. The fraction of the total fluence  $6.4 \cdot 10^{-4}$  ergs measured by *Beppo-SAX* between 40-700 keV that the PL components would account for is also reported. Numbers in bold are for the function used in [15].

scopes above the muon threshold determined by the detector depth, geometry and reconstruction capabilities, as observed in [35,36,37]. In order to derive the number of muons from a given photon spectrum we follow the analytical estimate in Ref. [38], that was checked against the Monte Carlo calculation in Ref [39]. We repeat here the main steps of that calculation. The muon spectrum from a differential photon spectrum  $\Gamma_0(E)$  is given by:

$$\frac{dN_{\mu}}{dE} = \Gamma_0(E) \frac{\epsilon_{\pi}}{E \cos \theta} \left( \frac{1 - r^3}{3(1 - r)} \right) z_{\gamma \pi} \frac{\Lambda_{\pi}}{\lambda_{\gamma N}} \left[ 1 + \ln \frac{t_{max}}{\Lambda_{\pi}} \right]$$
 (1)

where energies are in TeV,  $\theta$  is the zenith angle,  $r = m_{\mu}^2/m_{\pi}^2$  is the ratio of the squared muon and pion masses,  $\epsilon_{\pi} = 0.115$  TeV is the energy above which pion interaction dominates over decay. The pion flux at the atmospheric depth

t due to the photon flux  $\Gamma_0$  can be factorized as  $\pi(E,t) = \Gamma_0(E)\pi_2(t)$ , with  $\pi_2(t) = z_{\gamma\pi} \frac{\Lambda_{\pi}}{\lambda_{\gamma N}} (1 - e^{-t/\Lambda_{\pi}}) \sim z_{\gamma\pi} \frac{\Lambda_{\pi}}{\lambda_{\gamma N}}$ . The various terms are respectively: the z moment  $z_{\gamma\pi} = \frac{1}{\sigma_{\gamma N}} \int_0^1 dx x^{\alpha} \frac{d\sigma_{\gamma \to \pi}(x)}{dx}$ , that depends on the spectral index  $\alpha$  of the photon flux  $\frac{dN}{dE} \propto E^{-(\alpha+1)}$ ; the effective pion interaction length in the atmosphere  $\Lambda_{\pi}$ ; the interaction length associated with  $\pi$  photo-production  $\lambda_{\gamma N}$ . Following the discussion in Ref. [38] we assume:

$$z_{\gamma\pi} \frac{\Lambda_{\pi}}{\lambda_{\gamma N}} \sim \frac{1}{1 - z_{\pi\pi}} \sim \frac{A\sigma_{\gamma N}}{\sigma_{\pi A}} \times \langle nx \rangle_{\gamma \to \pi}$$
 (2)

with  $z_{\gamma\pi}=\frac{2}{3}$  and  $z_{\pi\pi}=\frac{2}{3}$  (this is the z moment for pion regeneration in the atmosphere). These values are suitable for hard spectra with  $\alpha$  around 1. We assume a constant pion photo-production cross-section  $\sigma_{\gamma N}\sim 0.1$  mb and an average mass number A=14.5 in the atmosphere. This is a reasonable assumbtion in the photon energy range  $\sim 0.1-10^2$  TeV  $[40,39]^{-2}$ . Moreover, we assume  $\sigma_{\pi A}\sim 198$  mb [38]. The logarithmic term in eq. 1 depends on  $t_{max}$ , the depth where the photon energy in the cascade has become too low to produce muons of energy E. It is assumed  $t_{max}=\lambda_R ln\left[\frac{E_{\gamma,max}< x_{\gamma\to\mu}>}{E}\right]$ , where  $\lambda_R$  is the radiation length in the atmosphere.  $E/< x_{\gamma\to\mu}>$  is the  $\gamma$  energy required to produce a muon of energy E and we assume  $< x_{\gamma\to\mu}>\sim 0.25$ . Moreover, in eq. 1 we have  $\frac{t_{max}}{\Lambda_{\pi}}=\frac{\lambda_R}{\Lambda_{\pi}}=(1-z_{\pi\pi})\frac{\sigma_{\pi A}}{\sigma_R}$  with  $\sigma_R\sim 480$  mb. The above muon flux is valid for energies large enough that muons do not decay, e.g. in our case, in which muons must have enough energy to survive underground.

The photon spectra motivated in Sec. 2.2 are expressed in the general form  $\Gamma_0(E) = \frac{dN}{dE} = \frac{F_{\gamma}}{E^{\alpha}} \cdot 10^{-12}$  with the units and parameters given in Tab. 3. We assume that the spectra we get from SGR 1900+14 data are similar for SGR 1806-20, a burst with similar features and duration. Because SGR 1806-20 is more energetic by over one order of magnitude, this represents another conservative estimate. Moreover, we recall that the measured values are lower limits on the fluence for both bursts. We assume that the photon spectrum extends to  $E_{\gamma,max}$  and in Tab. 4 we estimate the number of events for two values, 200 and 500 TeV, and show the number of signal events as a function of  $E_{\gamma,max}$  in Fig. 5. Photons of energies in excess of  $\sim$  500 TeV should be attenuated over galactic distances due to interaction on background photons. The minimum muon energy  $E_{\mu,min}$  that muons should have to cross the ice overburden depends on the inclination of the source respect to the detector. For AMANDA, located at the South Pole, a simple relation connects the zenith angle and the declination of the source, that is  $\theta = \delta + 90^{\circ} = 70^{\circ}$ . Being the

<sup>&</sup>lt;sup>2</sup> The resulting cross section from the FLUKA transport and interaction code [41] is in agreemet with this value of the  $\gamma N$  cross section, as well as data in Refs.[42] at GeV energies.

detector at a depth of 1500-2000 m, a muon induced by gammas from the source will have to transverse about 5.1 km of ice overburden before reaching the detector. We calculate the survival probability of muons with energy larger than 10 GeV at AMANDA depths using the MUM code for high energy muon energy losses [43]. In this calculation we account for the muon spectrum and the parent gamma spectrum in Tab. 3. Hence we derive the number of muons at AMANDA depth and for the given source zenith as:

$$N_{\mu} = \int_{E_{\mu,min}}^{E_{\mu,max}} \frac{dN_{\mu}}{dE} P_{surv}(depth, E_{\mu}) dE_{\mu}$$
(3)

assuming that  $E_{\mu,max} \sim \langle x_{\gamma \to \mu} \rangle E_{gamma,max} \sim 0.25 E_{\gamma,max}$ , for depth equal to 5.1 km.

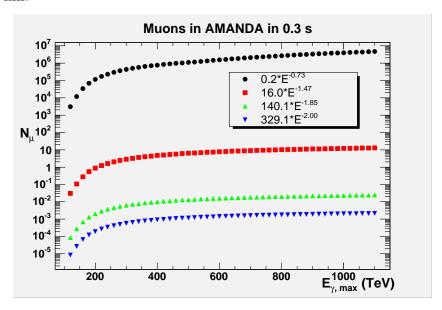


Fig. 5. Number of muons induced by gamma showers in 0.3 s for an almost horizontal area of  $30000 \text{ m}^2$  for a detector like AMANDA-II at a depth between 1.5-2 km for the 4 different photon sectra indicated and as a function of the maximum photon energy.

The main background source to the muons produced by gammas emitted in the flare are atmospheric muons. In the horizontal direction the atmospheric muon rate is reduced by roughly 2 orders of magnitude with respect to the vertical direction. Therefore the background is about 1 Hz. Furthermore, since the bulk of the energy is emitted in only 0.3 s from a point-like source, the background is limited to the time interval and the direction of the burst. Conservatively considering a search bin of 8°, well above the resolution of the detector and comparable to the size of the declination band [44] chosen by the experiment after a signal to noise optimization, the estimated background rate

from atmospheric muons is at the level of  $\pi(8*\pi/180)^2/(2\pi)\times 0.3\times 1=3\cdot 10^{-3}$  events in 0.3 s. Hence it is negligible.

Where the signal is concerned, we tabulate in Tab. 4 the expected number of muons from the burst in 0.3 s for  $E_{\gamma,max}=200$  TeV and 500 TeV. We assumed a near horizon effective area close to the geometrical area of AMANDA of about 30000 m<sup>2</sup>. The effective area includes cuts on the quality of the muon reconstruction, and was estimated for harder muon spectra than atmospheric muons for which an average value is 22000 m<sup>2</sup>. In Fig. 5 we show how the results vary for different  $E_{\gamma,max}$  values and for the 4 spectra we considered. Similar event rates might be observed by the future ANTARES detector, located at 2050-2400 m in the sea, that would be able to observe muons and showers induced by neutrinos from another flare from the source, SGR 1900+14, for more than 40% of a day. It will also be able to observe neutrino induced upward going muons and showers from SGR 1806-20.

As expected, the event rate is a strong function of the spectral index and of the normalization. In the absence of a possible detection, it is straightforward for AMANDA to constrain the high energy flux associated with the possibility that SGR's are high energy accelerators, possibly similar to GRB's.

$\mathbf{F}_{\gamma}$	Spectral	$\mu$ Events	Atmospheric	$\gamma$ showers
	Index	AMANDA	$\mu$ 's in AMANDA	in Milagro
$6.47 \cdot 10^{13}$	-0.73	$0.1 - 1 \cdot 10^6$	$3 \cdot 10^{-3}$	$1\cdot 10^{11}$
$9.42\cdot 10^8$	-1.47	0.8-6	$3\cdot 10^{-3}$	$8\cdot 10^4$
$3.13 \cdot 10^6$	-1.85	$0.1 - 1 \cdot 10^{-2}$	$4 \cdot 10^{-3}$	79
$3.29\cdot 10^5$	-2.00	$0.1 - 1 \cdot 10^{-3}$	$2\cdot 10^{-4}$	5

Table 4

The normalization of the  $\gamma$  flux and the spectral index for the giant flare. The normalization  $F_{\gamma}$  units are such that the differential flux  $\frac{dN}{dE} = F_{\gamma} \cdot (E/TeV)^{\alpha} \cdot 10^{-12}$  is in cm<sup>-2</sup> s<sup>-1</sup> TeV<sup>-1</sup>. The values of the *Beppo*-SAX fit are in bold. The corresponding number of muons in a detector like AMANDA-II of 30000 m<sup>2</sup> in 0.3 s is given. Two numbers are given in the third column: the smaller is obtained assuming a maximum photon energy of 200 TeV and the larger assuming 500 TeV. Also the atmospheric muon background in a search solid angular bin of 8° and in 0.3 s is indicated. The gamma shower events in Milagro in 0.3 s are also shown for a giant flare in its field of view (see the text).

# 3.1 Estimate of photon induced showers in Milagro

SGR 1806-20 was located above the Milagro horizon at the time of the Dec. 27 giant flare at a zenith angle of about 68°. The source might have been visible

for Milagro though we understand data at such zenith angle are not routinely analyzed by the experiment whose range covers 0-60 degrees. Nonetheless, we consider the effective area presented in [45,37] as function of the  $\gamma$  energy:  $A(E_{\gamma}) = 4 \cdot 10^6 (E/TeV)^{\beta}$  in cm<sup>2</sup>, where  $\beta = 1.39$  for  $E_{\gamma} > 1$  TeV and  $\beta = 2.35$  for  $E_{\gamma} \in [0.3, 1]$  TeV, and we use it for estimating the number of shower events in Milagro from an SGR burst eventually happening in a favorable sky region. Using the various gamma spectra we estimate event rates in Tab. 4 using the following formula:

$$\frac{N_{showers}}{T} = \int_{E_{\gamma,min=0.3TeV}}^{E_{\gamma,max}=100TeV} \frac{dN_{\gamma}}{dE_{\gamma}} \times A(E_{\gamma}) dE_{\gamma} \,. \tag{4}$$

For some of the spectral indexes Milagro may have seen a large signal during the first instants of the flare.

# 4 Neutrino initiated showers and upward-going muons from giant SGR flares

The photon fluxes previously discussed are accompanied by neutrinos because charged pions are produced at the source along with the neutral pions that decay into photons. Assuming that photons and neutrinos have this common origin, the neutrino spectrum can be derived from the photon spectrum by energy conservation along with simple kinematics [36,47]. Photons may cascade in the source to emerge with a steeper spectrum and they may even be absorbed, therefore only a lower limit on the neutrino flux can be derived using this technique.

It is likely that the target for neutrino production are the thermal photons surrounding the pulsar. We therefore assume  $p-\gamma$  interactions with the ambient radiation around the neutron star. There may also be a contribution from neutron decay from photo-disintegration of nuclei. The relation between the two spectra is:

$$\int_{E_{\gamma,min}}^{E^{\gamma,max}} E_{\gamma} \frac{dN_{\gamma}}{dE_{\gamma}} dE_{\gamma} = K \int_{E_{\nu,min}}^{E_{\nu,max}} E_{\nu} \frac{dN_{\nu}}{dE_{\nu}} dE_{\nu} , \qquad (5)$$

where K=1 for pp interactions and 4 for  $p-\gamma$ . In pp interactions charged and neutral pions are produced in equal numbers yielding 2  $\gamma$ 's carrying 1/2 of the neutral pion energy, that is 1/3 of the proton energy, and so  $E_{\gamma} \sim E_p/6$ . If muons also decay, there are 2 muon neutrinos per  $\gamma$  and so  $E_{\nu} \sim E_p/12$ . For

 $p-\gamma$  interactions, neutrinos and photons are produced from the  $\Delta$  resonance decay:  $p+\gamma \to \Delta \to n\pi^+ \to n\mu^+\nu_\mu \to ne^+\nu_e\bar{\nu}_\mu\nu_\mu$  and  $p+\gamma \to \Delta \to p\pi^0 \to p\gamma\gamma$ . Hence  $E_{\gamma,min}$  is determined by the threshold of the process for protons [47]:

$$E_p = \Gamma \frac{(2m_p + m_\pi)^2 - 2m_p^2}{2m_p} \sim \Gamma \times 1.23 GeV$$
 (6)

where we will consider a Lorenz factor  $\Gamma \sim 1$ . The minimum neutrino and photon energy are about 5% and 10%, respectively, of the proton energy  $(E_{\nu,min} = \langle x_{p \to \gamma} \rangle E_{p,min}/4$  and  $E_{\gamma,min} = \langle x_{p \to \gamma} \rangle E_{p,min}/2$ ), where  $\langle x_{p \to \gamma} \rangle \sim 0.2$  is the average fraction of proton energy transferred to pions). The maximum proton energy, and hence the maximum gamma and neutrino energies, depend on the kinematics in the beam that results from the burst. We will assume values a bit larger than what is calculated in Ref. [14]: here  $E_{p,max} \sim 100-300$  TeV [14], where protons are accelerated in the potential drop of the magnetar with surface magnetic field of  $\sim 10^{15}$  Gauss. As a matter of fact, we are considering giant flares and not the steady emission. Hence, we will assume here a maximum photon energy of 200 TeV and a maximum neutrino energy of 100 TeV. Also we assume that the photon spectra have the same spectral index, a very conservative assumption [37]. Using the  $\gamma$  spectra in Tab. 3, we obtain the neutrino fluxes in Tab. 5.

Neutrino Spectrum	Cascade events $(s^{-1})$			Upward-going $\mu$ 's
$({ m cm}^{-2} \ { m s}^{-1} \ { m GeV}^{-1})$	$ u_e$	$ u_{\mu}$	$ u_{ au}$	$(s^{-1})$
$5.90(E/GeV)^{-0.73}$	$1 \cdot 10^7$	$8 \cdot 10^6$	$1 \cdot 10^7$	$2 \cdot 10^6$
$8.74 \cdot 10^{-3} (E/GeV)^{-1.47}$	0.4	0.2	0.3	0.8
$3.09 \cdot 10^{-4} (E/GeV)^{-1.85}$	$9\cdot 10^{-5}$	$3\cdot 10^{-5}$	$6 \cdot 10^{-5}$	$5 \cdot 10^{-4}$
$8.23 \cdot 10^{-5} E^{-2.00}$	$3 \cdot 10^{-6}$	$1 \cdot 10^{-6}$	$2 \cdot 10^{-6}$	$3 \cdot 10^{-5}$

Table 5

Neutrino spectra obtained using the fluxes in Tab. 3 and eq. 5 and shower and upgoing-muon event rates in a detector like AMANDA-II per second for a source at  $\delta = \pm 20^{\circ}$ .

We use these fluxes to derive event rates for two different neutrino signatures: neutrino induced showers (cascade events), that have a  $4\pi$  coverage and can be observed even if the source is in the upper hemisphere of the detector and neutrino induced upward-going muons that can be observed only if the source is in the lower hemisphere; this is the case for SGR 1806-20 in the field of view of ANTARES and for SGR 1900+14 observable by AMANDA-II. We estimate event rates for AMANDA neutrino effective areas, though similar numbers apply for the present ANTARES detector design. Neutrino effective areas as a function of the energy for the declination of a source can be directly

convoluted with the neutrino spectra to provide event rates. To estimate the number of cascade events we have considered the AMANDA effective areas for neutrinos of all flavors presented in [48]. Because of oscillations, a cosmic neutrino beam reaches the Earth with equal fluxes for all flavors. For the near horizontal direction of the sources under consideration the absorption of neutrinos is almost negligible. To estimate upward-going neutrino event rates we used the effective area presented in [44]. Results are given in Tab. 5.

The background for neutrinos from the flare is due to atmospheric neutrinos and muons. As already explained in Sec. 3, it can be rejected using time and directional constraints. We neglect the contribution to the neutrino signal from the flare due to neutrinos that accompany muons from gammas considered in Sec. 3 because they would give a much smaller contribution to neutrinos directly produced at the source.

#### 5 Conclusions

Starting from measured spectra by *Beppo*-SAX for the SGR1900+14 giant flare, we have estimated the TeV gamma-ray and neutrino event rates expected (and possibly observed) for the AMANDA detector from SGR 1806-20 on Dec. 27, 2004. We showed that tight time and angular constraints can reduce the atmospheric muon background to negligible levels. The detectors are essentially free of background because of the time constraints.

A negative result will result in an interesting constraint on the possibility that SGR most intense flares are similar to small GRB's in our Galaxy.

## Acknowledgments

We thank Cristiano Guidorzi for helping us in understanding *Beppo*-SAX measurement and Igor Sokalski for providing us with underground muon survival probabilities. We also would like to thank the UW IceCupe group, and particularly Paolo Desiati and Albrecht Karle, for fruitful discussions.

#### References

[1] P. M. Woods and C. Thompson, Soft Gamma Repeaters and Anomalous X-ray pulsars: magnetar candidates, astro-ph/0406133, to appear in "Compact Stellar X-ray Sources", eds. W.H.G. Lewin and M. van der Klis.

- [2] For more information see also: R. C. Duncan's Web site: http://solomon.as.utexas.edu/duncan/magnetar.html
- [3] C. Kouveliotou et al., Ap. J. **510**(1999) L115.
- [4] V. M. Kaspi et al., Ap. J. **588**(2003) L93.
- [5] Milagro experiment Web site: http://www.physics.nyu.edu/~am3/milagro.html
- [6] Tibet Array Web site: http://www.icrr.u-tokyo.ac.jp/em/index-j.html
- [7] Lake Baikal experiment Web site: http://www.ifh.de/baikal/baikalhome.html
- [8] AMANDA experiment Web site: http://amanda.wisc.edu
- [9] IceCube experiment Web site: http://amanda.wisc.edu
- [10] ANTARES experiment Web site: http://antares.in2p3.fr
- [11] NEMO experiment Web site: http://nemoweb.lns.infn.it
- [12] KM3Net Web site: http://www.km3net.org
- [13] NESTOR experiment Web site: http://www.nestor.org.gr
- [14] B. Zhang et al., Ap. J. **595**(2003) 346.
- [15] M. Feroci et al., Ap. J. **515**(1999) L9.
- [16] See J. Borkowski *et al*, GCN 2920 circular at http://lheawww.gsfc.nasa.gov/docs/gamcosray/legr/bacodine/gcn3/2920.gcn3.
- [17] F. J. Vrba et al., Ap. J. **533** (2000) L17.
- [18] D. L. Kaplan et al., Ap. J. **556** (2001) 399.
- [19] Corbel and Eikenberry, A&A **419** (2004) 191.
- [20] D. Band et al., Ap. J. **413** (1993) 281.
- [21] W. Bednarek, MNRAS **302** (1999) 373.
- [22] D. F. Torres, E. Domingo-Santamaria, G. E. Romero, Ap. J. **601** (2004) L75.
- [23] L. A. Anchordoqui, H. Goldberg, F. Halzen and T. J. Weiler, Phys. Lett. B593 (2004) 42.
- [24] W. Bednarek, F. Burgio and T. Montaruli, New Astron. Rev. 49 (2005) 1.
- [25] E. Nakar, T. Piran, R. Sari, Giant Flares as Mini Gamma-Ray Bursts, e-print: astro-ph/0502052.
- [26] See E. P. Mazets et al, GCN 2922 circular at http://lheawww.gsfc.nasa.gov/docs/gamcosray/legr/bacodine/gcn3/2922.gcn3

- [27] See S. Boggs *et al*, GCN 2936 circular at http://lheawww.gsfc.nasa.gov/docs/gamcosray/legr/bacodine/gcn3/2936.gcn3
- [28] E. P. Mazets et al., Astr. Lett. **25** (1999) 635.
- [29] M. Feroci, K. Hurley, R. C. Duncan and C. Thompson, Ap.J. 549 (2001) 1021.
- [30] C. Guidorzi et al., A&A 416 (2004) 297.
- [31] A. I. Ibrahim et al., Ap. J 558 (2001) 237.
- [32] G. J. Lenters et al., Ap. J. **587** (2003) 761.
- [33] E. Kellogg, J. R. Baldwin and D. Kock, Ap. J. 199 (1975) 299.
- [34] C. Guidorzi, private communication.
- [35] F. Halzen, T. Stanev, G. B. Yodh, Phys. Rev. **D55** (1997) 4475.
- [36] J. AlvarezMuniz and F. Halzen, Ap. J. **521** (1999) 928.
- [37] F. Halzen and D. Hooper, JCAP 0308 (2003) 006.
- [38] M. Drees, F. Halzen, and K. Hikasa, Phys. Rev. **D39** (1989) 1310
- [39] T. Stanev, T. K. Gaisser and F. Halzen, Phys. Rev. **D32** (1985) 1244.
- [40] G. Battistoni private communication
- [41] FLUKA Web Site: http://www.fluka.org
- [42] V. Muccifora et al., Phys. Rev. C60 (1999) 064616 and Bianchi et al., Phys. Rev. C60 (1999) 064616.
- [43] I.A.Sokalski, E.V.Bugaev, S.I.Klimushin, Phys. Rev. D64:074015 (2001) and Igor Sokalski private communication.
- [44] M. Ackermann et al., Search for extra-terrestrial point sources of high energy neutrinos with AMANDA-II using data collected in 2000-2, subm. to Phys. Rev. Lett. and astro-ph/0412347 and J. Ahrens et al., Phys. Rev. Lett. **92** (2004) 071102.
- [45] R. Atkins et al., Status of the Milagro Gamma-Ray Observatory, Proc. of 27<sup>th</sup> Int. Cosmic Ray Conference and e-Print Archive: astro-ph/0110513
- [46] J. Alvarez-Muniz and F. Halzen, Ap. J. **576** (2002) L33.
- [47] High Energy Neutrinos from the TeV Blazar 1ES 1959+650,e-print: astro-ph/0502449.
- [48] M. Ackermann et al., Astrop. Phys. 22 (2004) 127.